HHS Public Access

Author manuscript

Adv Funct Mater. Author manuscript; available in PMC 2021 October 01.

Published in final edited form as:

Adv Funct Mater. 2020 October 1; 30(40): . doi:10.1002/adfm.202002031.

Promoting Cell Migration and Neurite Extension along Uniaxially Aligned Nanofibers with Biomacromolecular Particles in a Density Gradient

Jiajia Xue, **Tong Wu**, **Jichuan Qiu**, **Sarah Rutledge**, **Michael L. Tanes**

The Wallace H. Coulter Department of Biomedical Engineering Georgia Institute of Technology and Emory University, Atlanta, GA 30332, USA

Younan Xia

The Wallace H. Coulter Department of Biomedical Engineering Georgia Institute of Technology and Emory University, Atlanta, GA 30332, USA

School of Chemistry and Biochemistry, School of Chemical and Biomolecular Engineering Georgia Institute of Technology, Atlanta, GA 30332, USA

Abstract

A simple method based upon masked electrospray is reported for directly generating both unidirectional and bidirectional density gradients of biomacromolecular particles on uniaxially aligned nanofibers. The method has been successfully applied to different types of biomacromolecules, including collagen and a mixture of collagen and fibronectin or laminin, to suit different types of applications. Collagen particles in a unidirectional or bidirectional gradient are able to promote the linear migration of bone marrow stem cells or NIH-3T3 fibroblasts along the direction of increasing particle density. In the case of particles made of a mixture of collagen and fibronectin, their deposition in a bidirectional gradient promotes the migration of Schwann cells from two opposite sides toward the center, matching the scenario in peripheral nerve repair. As for a mixture of collagen and laminin, the particles in a unidirectional gradient promote the extension of neurites from embryonic chick dorsal root ganglion in the direction of increasing particle density. Taken together, the scaffolds featuring a combination of uniaxially aligned nanofibers and biomacromolecular particles in density gradient can be applied to a range of biological studies and biomedical applications.

Keywords

biomacromolecular particles; cell migration; electrospun fibers; gradient; neurite extension

younan.xia@bme.gatech.edu.

The ORCID identification number(s) for the author(s) of this article can be found under https://doi.org/10.1002/adfm.202002031.

Supporting Information

Supporting Information is available from the Wiley Online Library or from the author.

Conflict of Interest

The authors declare no conflict of interest.

1. Introduction

One of the key strategies for tissue repair or regeneration is to recruit appropriate cells to the injured site through guided migration for the acceleration of healing.[1,2] For example, skin regeneration requires the re-establishment of dermis, which can be augmented by stimulating and directing fibroblasts to migrate from the healthy tissues in the surroundings to the wound site.[3] As for the repair of periphery nerve injury, it requires not only the recruitment of glial cells to the defect site but also the promotion of neurite extension and axon regrowth.[4] In this case, a scaffold capable of promoting cell migration and neurite extension will work the best in improving the efficacy of repair.[5,6]

As a potent topographic cue, the structural features on the surface of a scaffold have been widely explored for guiding the migration of cells and extension of neurites through a process known as contact guidance.[7] In the presence of an oriented extracellular matrix (ECM), the leader cells can become highly polarized during the migration of collective cells, inducing and promoting directional migration.[8] Similarly, the growth cones of neurites can also sense the topographic cue for the initiation and continuation of directional extension. In practice, engineered substrates with anisotropic topographic cues, including those presented by grooves,[9] pillars,[10] and fibers,[11] have been explored to direct the migration of various types of cells and the extension of neurites. In addition to the topographic features, the biochemical properties of a scaffold can also be leveraged to control the behavior of cells. In particular, the haptotactic cue arising from the gradient in a substrate-bound factor has been used to direct cell migration and neurite extension through a steering mechanism in responding to the asymmetric environmental factor.[12–14] In this regard, many methods have been developed to functionalize the surface of a scaffold with haptotactic cues in the form of ECM proteins, bioactive factors,[15] particles,[16–18] and even cells.[19]

Among various types of scaffolding materials, electrospun nanofibers have been extensively explored for tissue repair or regeneration owing to their capability to mimic some structural and compositional features of ECM and to combine the topographic and haptotactic cues in one scaffold.[20–23] The nanofibers can be easily collected as a uniaxially aligned array, providing a topographic cue to guide and accelerate cell migration and neurite extension along the direction of alignment.[24,25] For example, with the use of uniaxially aligned nanofibers, fibroblasts were able to move rapidly across an artificial wound field, accelerating the wound closure.[26] As another typical example, nerve guidance conduits constructed with uniaxially aligned fibers greatly promoted axon regrowth relative to the case of random fibers.[27,28] A gradient of bioactive agents can also be further combined with the uniaxially aligned nanofibers, offering a haptotactic cue to further improve the guidance efficacy.[15,29–31] For example, a gradient of proteins was generated on a mat of aligned nanofibers by varying the contact time between the bioactive agents and the fibers.[15,29–31] In other studies, chemical reactions such as surface-initiated atom transfer radical polymerization have been used to produce a gradient of peptides on the surface of fibers.[32–34] These methods, however, typically involve the use of multiple steps and custom-made reagents, limiting their capability and versatility. In this regard, a simple and effective method remains to be developed for large-scale production of haptotactic cue in a gradient

manner to work together with the topographic cue for maximizing cell migration and neurite extension.

As an important electrohydrodynamic process but a variant of electrospinning, electrospray is a simple and versatile method for depositing particles on a substrate, which can be readily combined with an electrospinning process.[35] It has been successfully applied to produce micro/nano-particles from a wide variety of biomacromolecules, including collagen, gelatin, and chitosan, as well as their mixtures.[36] As the major component of ECM, collagen has been extensively studied and is considered one of the most important biomacromolecules in affecting cell adhesion and migration.[37,38] Other ECM components, such as laminin and fibronectin, can also be incorporated into the scaffolds to better mimic the native ECM in terms of (bio)chemical composition. These biomacromolecules play a vital role in cell adhesion, as well as migration and differentiation. For example, laminin can effectively enhance axonal regrowth for some sensory neurons, contributing to peripheral nerve repair.[39] Fibronectin is involved in the migratory pathways of Schwann cells in the peripheral nervous system.[40] By spatially varying the deposition time with the use of a moving mask, a unidirectional gradient of particles can be readily fabricated on a flat substrate.[41] In principle, a scaffold that simultaneously presents topographic and haptotactic cues can be fabricated by depositing the electrosprayed biomacromolecular particles, with a gradient in coverage density, on a mat of uniaxially aligned nanofibers. Such a scaffold will present a unique integration of the topographic cue arising from the uniaxially aligned nanofibers and a haptotactic cue enabled by the particles in a density gradient.

Here we report a method that combines masked electrospray and electrospinning for the direct deposition of biomacromolecular particles on uniaxially aligned nanofibers in both unidirectional and bidirectional density gradients. We then apply these graded scaffolds to investigate their impact on cell migration and neurite extension. We first examine the migration of bone marrow stem cells or NIH-3T3 fibroblasts on a scaffold consisting of uniaxially aligned nanofibers functionalized with collagen particles in unidirectional or bidirectional density gradient. We also demonstrate the potential use of such graded scaffolds for applications in peripheral nerve repair. We fabricate a bidirectional gradient in coverage density for particles made of a mixture of collagen and fibronectin and then evaluate their influence on the migration of Schwann cells from two opposite sides toward the center. By changing fibronectin to laminin, we further fabricate a unidirectional density gradient of the particles for augmenting the directional outgrowth of neurites from embryonic chick dorsal root ganglion (DRG).

2. Results and Discussion

2.1. Fabrication of Density Gradients of Particles on Aligned Nanofibers

Figure 1 shows a schematic of the technique, in which the deposition of electrosprayed particles is intervened by a movable mask to produce a gradient in coverage density along the moving direction. For the particles sprayed from a spinneret, they are supposed to be uniformly distributed across the surface of a collector, with the coverage density being directly proportional to the deposition time. By linearly moving the mask placed between the spinneret and the collector to control the deposition time, a unidirectional gradient in

coverage density will be obtained. Similarly, a bidirectional gradient that increases from two opposite sides to the center can also be fabricated by completely blocking half of the collector while conducting the masked deposition, followed by the masked deposition on the other half. The physical properties of the electrospray solution and the operation parameters such as the moving speed of the mask can all be adjusted to alter the gradient.

We initially focused on collagen, a major component of ECM that is considered one of the most important biomacromolecules in affecting cell adhesion and migration. Figure S1A–C (Supporting Information) shows the scanning electron microscopy (SEM) images of a typical sample of the collagen particles at different magnifications, which are deposited on a silicon wafer. In principle, the electrosprayed droplets should take a spherical shape in order to minimize the total surface energy. If most of the solvent is evaporated before the particles touch the collector, the particles can take a more or less spherical shape, as demonstrated in a previous study by atomic force microscopy (AFM) imaging for poly(lactic-*co*-glycolic acid) (PLGA).[41] However, if a large amount of solvent remains in the droplets before they are deposited onto the collector, the gel-like droplets will be deformed to take a nonspherical shape.[42,43] Based on the SEM images, this seems to be the case for the particle with a relatively large size and thus the involvement of a large amount of solvent. In general, the shape or morphology of the electrosprayed particles can be tailored by adjusting the properties of the polymer solution, especially its concentration and conductivity.

Overall, the particles showed an average diameter of 395 ± 86 nm by measuring 100 particles in the SEM images of three samples (Figure S1D, Supporting Information). The size of the particles can be tuned by adjusting the properties of the collagen solution, including its concentration and the composition of the acetic acid solution for dissolving collagen, or the processing parameters, such as the flow rate and the field strength.[43] Specifically, the size of the particles can be increased by increasing the concentration or the flow rate of the solution. Monodispersity can be improved by increasing the polymer concentration and thus viscosity and reducing the flow rate or the conductivity of the polymer solution.[43]

We introduced a physical mask, moving linearly at a speed of 0.1 cm min^{-1}, to spatially alter the collection time and thus the coverage density of collagen particles deposited on an array of uniaxially aligned polycaprolactone (PCL) nanofibers. Figure 2 shows SEM images of the aligned nanofibers after being functionalized with collagen particles in a density gradient for a total duration of 20 min. The pristine PCL nanofibers showed a smooth surface, together with an average diameter of 583 ± 112 nm (Figure 2A,B). As the collection time was increased, more collagen particles were deposited on the surface of the nanofibers (Figure 2C–F). In the region corresponding to a collection time of 20 min, the surface of the nanofibers was covered by a high density of collagen particles, as marked by red dotted ellipses, together with arrows, in Figure 2F. From the image, the deposited particles were more or less fused together with the surface of the nanofibers without additional treatment because of the presence of some residual solvent in the particles. Since the only difference between the samples shown in Figure 2B,D,F, was the duration of time used for collecting the particles electrosprayed from the same collagen solution, the particles (i.e., bumps) presented on the surface of the nanofibers should be made of collagen only.

In a separate experiment, two samples of PCL nanofibers were uniformly deposited with collagen particles by electrospray for 10 and 20 min, and the water contact angle of the PCL nanofiber mat decreased from 125° to 29° and 11°, respectively, because of the hydrophilicity of collagen. This result further confirms those particles were made of hydrophilic collagen rather than some beads that may be generated during the electrospinning of PCL solution because PCL is a very hydrophobic polymer. After solidification, the particles would not be able to move and aggregate because they stuck to the surface of the nanofibers. In addition, collagen has a high glass transition temperature and the polymer chains should not be moveable at room temperature.[44,45] The stability of the particles on the surface of the nanofibers is also important for long-term culture and in vivo implantation. To this end, in situ monitoring of the size and even morphology of the particles will be required before this system is applied to a long-term application that lasts for up to 1 month.[46]

We also fabricated a gradient in coverage density for collagen particles loaded with fluorescein isothiocyanate-labeled bovine serum albumin (FITC-BSA). Such a sample allowed us to quantify the gradient by fluorescence microscopy imaging. Figure 3A shows the plots of relative fluorescence intensities as a function of distance along the aligned fibers when the FITC-BSA-loaded collagen particles were deposited in uniform and unidirectionally graded distributions, respectively. The gradient could be readily maneuvered by varying the moving speed of the mask and thereby the spatial variations in terms of collection time. A greater slope was obtained when the moving speed was reduced from 0.10 to 0.067 cm min^{-1}, leading to a more significant difference in fluorescence intensity at the two opposite sides of the mat. Figure 3B shows a sample with a bidirectional gradient in particle density and thus an increase in fluorescence intensity from the two opposite sides of the mat to the center, along the fiber alignment. In addition to the continuous gradients, we could also generate a step gradient by programming the speed at which the mask moves. Taken together, integration of electrospray with a moving mask placed over the collector offers a simple and viable method for depositing biomacromolecular particles with a gradient in coverage density. A variety of payloads can also be incorporated into the particles during the electrospray process. Furthermore, by changing the solution for electrospray, it is expected that particles made of different polymers or other types of materials can be codeposited on the same substrate.

2.2. Unidirectional Migration of Bone Marrow Stem Cells

Harnessing chemokine signaling can increase the number of endogenous stem cells recruited to the site of injury or damaged tissue.[47,48] For example, endogenous bone marrow stem cells can migrate to the bone damage site and participate in the formation of new bone.[49] As a major component of ECM, collagen acts not only as a framework for structural support of tissue but also as a substance for regulating the behaviors of stem cells, including adhesion, migration, and differentiation. Therefore, we chose collagen as a material for the bioactive particles to examine their impact on the behavior of bone marrow stem cells.

Figure 4A and Figure S2 (Supporting Information) show the fluorescence micrographs of bone marrow stem cells on different types of nanofiber scaffolds and tissue culture plate

(TCP), respectively. These images were recorded from fixed cells. Ideally, fluorescence micrographs recorded at day 0 would be helpful in resolving the starting point for cell migration but we had to wait until the end of an experiment before the cells could be fixed. Nevertheless, the edge (i.e., the starting point) of the seeded cells could be easily marked. We could also resolve the boundary between the seeding zone and migration zone by leveraging the difference in cell density between these two regions. The cells tended to migrate along the nanofibers with a uniaxial alignment while undergoing random migration on TCP or a mat of random nanofibers. On the scaffolds consisting of aligned nanofibers functionalized with collagen particles in a unidirectional gradient (AF-G), the cells migrated to the farthest distance (4.57 ± 0.79 mm) in comparison with those on the scaffolds consisting of either aligned nanofibers coated with collagen particles in a uniform distribution (AF-U) (3.61 ± 0.54, $P < 0.01$) or aligned nanofibers only (AF) (1.47 ± 0.86 mm, $P < 0.01$). As shown in Figure 4B, the scaffold consisting of pristine aligned nanofibers also resulted in a longer migration distance for the collective cells when compared with both the scaffold consisting of pristine random nanofibers and TCP.

We divided the migration zone into four regions with a 1 mm incremental increase along the fiber alignment and counted the number of cells over an area of 1 mm^2 in each region. Figure 4C compares the numbers of cells on different types of scaffolds. We observed a large number of cells in the entire area of the four regions when the cells were seeded on the graded scaffold AF-G, but significantly fewer cells in the migration zones for the scaffold coated with collagen particles in a uniform distribution ($P < 0.01$). In addition, compared with pristine aligned nanofibers, the scaffolds coated with collagen particles, regardless of the pattern of distribution, showed a better performance in promoting the migration of bone marrow stem cells ($P < 0.01$). These results indicate that the contact guidance from the aligned nanofibers and the collagen particles with a density gradient worked synergistically to promote the migration of stem cells toward the region with an increased density of particles. Figure S3 (Supporting Information) shows fluorescence micrographs of cells, at a higher magnification, in the migration zones of different types of scaffolds. The cytoskeleton took an elongated morphology and was greatly extended on the uniaxially aligned nanofibers while showing a random arrangement and less extension on random nanofibers. The cells were able to sense the guidance from both the uniaxial alignment of the nanofibers and the gradient of collagen particles, taking an elongated orientation while migrating toward the direction with increasing particle density. In this process, haptotaxis, which refers to the directional movement of cells in response to substrate-bond factors, is triggered by the particle gradient. The initial response of cells to a gradient is polarization, by which chemosensory signaling receptors will be redistributed.[50] If cellular polarization persists in one direction, cell migration will occur in succession.

It should be pointed out that when the cells were cultured on the scaffolds for 3 days, they could also undergo division, in addition to migration. To exclude the influence of cell proliferation, one can perform the cell migration assay in a medium without serum or with no more than 1% of serum but usually for no longer than 24 h. In addition to serum starvation, cytosine arabinoside (a DNA synthesis inhibitor) or mitomycin C (a mitosis inhibitor) can also be added to inhibit cell proliferation. Alternatively, the time-lapse method can be used to follow the movement of the same cell on the scaffold. If the cell divides

during the study, only one of the new cells will be traced.[51,52] In this study, since the control groups were also cultured under the same conditions, the impact of cell division could be more or less neglected.

2.3. Bidirectional Migration of NIH-3T3 Fibroblasts

Scaffolds made of uniaxially aligned nanofibers can promote wound closure by inducing the directional migration of repairing cells such as fibroblasts.[53] By further introducing a gradient of immobilized biomacromolecules onto the surface of the nanofibers, the migration of repairing cells toward the wound bed can be accelerated to promote the reconstruction of new tissue and improve wound healing. Here we also demonstrate the feasibility of using masked electrospray to fabricate a bidirectional gradient in coverage density of biomacromolecular particles on a scaffold of uniaxially aligned nanofibers, with the density increasing from the two opposite sides to the center. We also focused on collagen for its positive role in regulating the migration of fibroblasts. To study the combined effect from the uniaxial alignment and the gradient in particle density, we analyzed the migration of NIH-3T3 fibroblasts from two opposite sides toward the center of a scaffold comprised of uniaxially aligned nanofibers functionalized with collagen particles in a bidirectional gradient. Control groups included aligned nanofibers deposited with the collagen particles in a uniform distribution, as well as scaffolds made of pristine random and aligned nanofibers.

We placed a polydimethylsiloxane (PDMS) strip at the center of the scaffold to generate a 6 mm “wound,” toward which the NIH-3T3 fibroblasts were supposed to migrate from the two opposite sides. Figure 5 and Figure S4 (Supporting Information) show fluorescence micrographs of the fibroblasts on different types of nanofiber scaffolds consisting of pristine random nanofibers, pristine aligned nanofibers, aligned nanofibers functionalized with collagen particles in a uniform distribution or a bidirectional density gradient. Again, the fibroblasts tended to migrate along the nanofibers with a uniaxial alignment while they migrated haphazardly on the random nanofibers. On the scaffold consisting of aligned nanofibers functionalized with collagen particles in a bidirectional gradient (AF-G), the cells almost covered the entire region of the migration zone. However, a void was left behind for the cells cultured on the scaffold made of aligned nanofibers and coated with collagen particles in a uniform distribution (AF-U), even though the cells were connected to each other. Very few cells were observed in the central regions of the scaffolds made of pristine random and aligned nanofibers.

We divided the migration zone into six regions with a 1 mm incremental increase along the fiber alignment. Figure 5B compares the numbers of cells over an area of 1 mm^2 in each region of the different types of scaffolds. Compared with the pristine aligned nanofibers, the presence of the collagen particles significantly increased the number of cells in each region of the migration zones. When the cells were cultured on the graded scaffold AF-G, more cells were found in each region relative to the case when the cells were cultured on the uniform scaffold AF-U ($P < 0.01$). In addition, the cells could migrate to a farther distance when cultured on the aligned nanofibers relative to the case of random nanofibers ($P < 0.01$) (Figure 5C). The morphologies of fibroblasts in the migration zones on different types of scaffolds could be seen from fluorescence micrographs in Figure S5 (Supporting

Information), at a high magnification. These results indicate that the migration of fibroblasts from the two opposite sides toward the center could be accelerated by combining the contact guidance from the uniaxially aligned nanofibers and the bidirectional gradient of the collagen particles. Once the cells had met at the midpoint, the graded surface would be completely covered by cells, and the cells would then undergo proliferation and/or differentiation rather than migration. This type of graded scaffold can be leveraged to promote the migration of repairing cells in an effort to promote the wound healing process.

2.4. Bidirectional Migration of Schwann Cells

Following an injury in the peripheral nervous system, the denervated Schwann cells not only provide a trophic support but also dedifferentiate, proliferate, and migrate to the wounded area to form the bands of Büngner, encouraging axon regrowth and nerve regeneration.[54,55] To simulate this scenario, we also fabricated a bidirectional density gradient of biomacromolecular particles on a scaffold made of uniaxially aligned nanofibers, with the density increasing from the two opposite sides to the center. As such, we were able to mimic the migration of Schwann cells from both the proximal and distal ends of the served nerve toward the center of the injured site. We added fibronectin into collagen for its crucial involvement in the migratory pathways of Schwann cells in the peripheral nervous system.[40] Figure S6 (Supporting Information) shows SEM images of aligned nanofibers functionalized with electrosprayed particles made of a mixture of collagen and fibronectin, indicating no significant difference with the samples involving particles made of pure collagen.

Using a similar method as described above, we placed a PDMS strip at the center of the scaffold to generate a 6-mm “injury,” toward which the Schwann cells were supposed to migrate from the two opposite sides. Figure 6A and Figure S7 (Supporting Information) show fluorescence micrographs of Schwann cells on the different types of scaffolds. Similarly, we divided the migration zone into six regions with a 1 mm incremental increase along the fiber alignment. Figure 6B compares the numbers of cells over an area of 1 mm^2 in each region of the different types of scaffolds. Compared with the pristine aligned nanofibers, the presence of the electrosprayed particles significantly increased the number of cells in the center region of the migration zones. When the cells were cultured on the graded scaffold, more cells were found in regions II and V relative to the case of uniform scaffold ($P < 0.01$). In addition, the Schwann cells could migrate to a farther distance when cultured on the aligned nanofibers relative to the case of random nanofibers. Furthermore, the cells cultured on the graded scaffold could reach regions III and IV, significantly farther than those cultured on the uniform scaffold and on the pristine aligned nanofibers ($P < 0.01$) (Figure 6C). Figure S8 (Supporting Information) shows the fluorescence micrographs at a high magnification, revealing the morphologies of the cells in the migration zones of the different types of scaffolds. Through interactions with the surroundings, the Schwann cells could sense the contact guidance from the uniaxially aligned nanofibers and the bidirectional gradient of the particles, taking an elongated orientation and migrating toward the direction with increasing particle density. After rolling up the graded scaffold to form a tubular conduit, this unique feature can be leveraged to promote the migration of endogenous

Schwann cells in an effort to enhance axon elongation for promoting the repair of peripheral nerve injury.[27,28]

2.5. Extension of Neurites from DRG

For the repair of peripheral nerve injury, the directional extension of neurites is critical to the reconnection of the proximal and distal ends of the severed nerve for the restoration of nerve function.[56] Uniaxially aligned nanofibers have been used to construct nerve guidance conduits for promoting the unidirectional extension of neurites.[27,28] With the integration of gradients in chemical cues, the directional extension of neurites can be further augmented.[14,15] Compared with other types of ECM components, laminin can effectively enhance axonal regrowth for some sensory neurons.[39] As such, we added laminin into collagen particles to investigate the combined effect of topographic and hypotactic cues on the extension of neurites. Using masked electrospray, we generated a unidirectional gradient in coverage density for particles made of a mixture of collagen and laminin on a scaffold made of uniaxially aligned nanofibers. Figure S9 (Supporting Information) shows SEM images of the aligned nanofibers functionalized with the electrosprayed particles, indicating no significant difference with the samples involving particles made of pure collagen or a mixture of collagen and laminin.

An embryonic chick DRG body was seeded at the center of each type of scaffold, including those consisted of pristine aligned nanofibers, and aligned nanofibers functionalized with the particles in a uniform distribution or a unidirectional density gradient. Figure 7A shows fluorescence micrographs of neurites projecting from the DRG bodies after incubation for six days. Figure S10 (Supporting Information) shows the images at a higher magnification to reveal the morphology of the neurites more clearly. Figure 7B,C compares the average and longest lengths of neurites extending from the left and right sides of the DRG bodies. In all cases, the neurites were projected along the direction of the fiber alignment because of the contact guidance. When seeded on the scaffold functionalized with the particles, the growth cones of the neurites could recognize the ECM macromolecules and be motivated to reach out for the next particles. Furthermore, the particles could enhance the adherence of growth cones to the surface of the scaffold, promoting the extension of neurites. Therefore, the lengths of neurites extending from the DRG cultured on the uniform scaffold were significantly longer relative to the case of pristine aligned nanofibers ($P < 0.01$). There was no significant difference for the length of neurites extending from the two different sides of the DRG when cultured on the uniform scaffold. In contrast, when the DRG was cultured on a scaffold featuring a particle gradient increasing from the left to the right side along the fiber alignment, as indicated by the white arrow in Figure 7A, the longest length of the neurites on the right side of the DRG was 2265 ± 46 μm, significantly longer than that on the left side (1635 ± 16 μm, $P < 0.01$). Meanwhile, the average and the longest lengths of the neurites were significantly increased when the particles were switched from a uniform to a graded distribution. The growth cones of the neurites could sense and respond to the content increase in the attractive biomacromolecules to further expand its membrane along the direction with increasing particle density. Taken together, it can be concluded that the directional extension of neurites could be greatly enhanced by combining the topographic

and haptotactic cues. This strategy can be utilized to modify the inner surface of a nerve guidance conduit in an effort to further improve nerve regeneration.

2.6. Discussion

The results presented above demonstrate that a scaffold can be fabricated to simultaneously present topographic and haptotactic cues by coating a mat of uniaxially aligned nanofibers with biomacromolecular particles in a density gradient. The topographic cue offered by the aligned nanofibers and the haptotactic cue arising from the density gradient can work synergistically to accelerate cell migration and promote neurite extension. As expected, any variation in the particle density gradient will affect the migration of cells. In addition, when the nanofibers are uniformly coated with particles made of collagen (or other biomacromolecules), the difference in the amount of the deposited particles can also affect the migration of cells because of the hydrophilicity and bioactivity of collagen (or other biomacromolecules). At the same time, the surface roughness of the as-obtained fibers will be changed with the deposition of particles, which will introduce another factor that can influence the cell behavior. Taken together, the mechanism responsible for the migration of cells on the particle-coated nanofibers can be a complicated one, which deserves a systematic study in the future. The optimization of the size and shape of the particles, as well as the slope of the gradient also needs to be investigated systematically in the future to maximize the efficacy of such a scaffold in promoting cell migration and neurite extension. In addition to studying the migration of collective cells, the migration speeds of individual cells should also be evaluated by monitoring their movement on the different types of scaffolds for the achievement of a quantitative understanding of the migration process.

3. Conclusion

We have demonstrated the feasibility of using masked electrospray to directly fabricate both unidirectional and bidirectional density gradients of biomacromolecular particles on uniaxially aligned nanofibers. This method has been successfully applied to different types of biomacromolecules from the ECM in targeting different types of applications. Specifically, collagen particles in a unidirectional gradient promoted the migration of bone marrow stem cells in the direction of increasing particle density, which can be potentially applied to promote tissue regeneration by recruiting the endogenous stem cells to the defect sites. In another demonstration, collagen particles in a bidirectional gradient accelerated the migration of NIH-3T3 fibroblasts from two opposite sides toward the center for use in wound closure. In targeting a potential application in peripheral nerve repair, aligned nanofibers coated with the particles consisting of a mixture of collagen and fibronectin in a bidirectional gradient could promote the migration of Schwann cells from two opposite sides toward the center. Regarding neurite extension, the particles made of a mixture of collagen and laminin in a unidirectional gradient enhanced the extension of neurites from a DRG body in the direction of increasing particle density. As a major advantage, this method can be readily applied to many other types of nanofiber mats, including those consisting of aligned or random fibers made of different polymers because the deposition method depends on neither the orientation of the fibers nor the type of the polymer. To this end, scaffolds can be constructed for a variety of biomedical applications such as bone regeneration, wound

healing, and peripheral nerve repair by switching to different combinations of materials, composition of the particles, and the type of gradient for the particles.

4. Experimental Section

Chemicals and Materials:

PCL ($M_w \approx 80\,000$ g mol^{-1}), dichloromethane, *N,N*-dimethylformamide, and Type IV collagen were purchased from Sigma-Aldrich. All other chemicals including Dulbecco's modified Eagle's medium (DMEM), α-MEM, fetal bovine serum (FBS), antibiotic antimycotic (ABAM), Hank's buffered salt solution (HBSS), phosphate buffered saline (PBS, pH 7.4), laminin from mouse, human plasma fibronectin, and antibodies were purchased from Thermo Fisher Scientific. The water used in all experiments was obtained by filtering through a set of Millipore cartridges (Epure, Dubuque, IA).

Electrospinning of Nanofibers:

PCL nanofibers were fabricated by electrospinning using a traditional setup. A PCL solution at a concentration of 10 wt% was prepared by dissolving PCL pellets in a mixture of dichloromethane and *N,N*-dimethylformamide at a volume ratio of 80:20. The solution was then fed through a 22 gauge blunt needle at a rate of 1.0 mL h^{-1}. Afterwards, a high voltage (DC) of 15 kV was applied between the tip of the needle and a grounded collector. A stainless-steel, U-shape frame (with an opening of 2 cm × 5 cm) or a piece of glass coverslip (2.2 cm × 2.2 cm) was used as the collector to separately collect uniaxially aligned or random nanofibers. After electrospinning for 30 min, the high voltage was terminated. The uniaxially aligned nanofibers deposited on the frame were transferred and affixed on a glass coverslip (2.2 cm × 2.2 cm) using a medical silicone adhesive.

Electrospray of Particles:

A collagen solution at a concentration of 20 mg mL^{-1} was prepared by dissolving collagen in 70% aqueous acetic acid (v/v). Electrospraying was then performed using the similar setup to electrospinning except that a piece of aluminum foil served as the collector. The collagen solution was pumped out through the blunt needle at a feeding rate of 0.5 mL h^{-1}, and a high voltage (DC) of 20 kV was applied between the tip of the needle and the collector. A silicon wafer cleaned by ethanol was also placed on the aluminum foil to collect the electrosprayed particles for SEM characterization. The average diameter of the particles was measured from 100 particles in three SEM images.

Deposition of Particles on the Electrospun Nanofibers:

Scaffolds consisting of uniaxially aligned nanofibers covered by collagen particles in a uniform distribution were fabricated by directly electrospraying the particles onto the nanofibers. The gradient counterpart was obtained using a masked electrospraying technique. Briefly, a physical mask was connected to a second syringe pump and placed 1 cm above the mat of uniaxially aligned nanofibers during electrospraying. The mask was then controlled to move linearly at a constant speed of 0.1 cm min^{-1} to spatially alter the collection time of the particles on the mat. After collecting for a total duration of 20 min, the particles were deposited on the mat with a unidirectional gradient in the coverage density.

The slope of the unidirectional gradient was also altered by decreasing the moving speed of mask to 0.067 cm min^{-1} for a total collecting duration of 30 min. A bidirectional gradient in the coverage density that increasing from two opposite sides to the center was fabricated by completely blocking half of the collector while conducting the masked deposition, followed by deposition on the other half. FITC-BSA, fibronectin, or laminin were also incorporated into the collagen particles by electrospraying the collagen solutions containing 5 mg mL^{-1} for FITC-BSA or 100 μg mL^{-1} for fibronectin and laminin. The obtained samples were then placed into the wells of a six-well plate, sterilized under UV for 30 min, and then stored at 4 °C until further use.

Characterization of Nanofibers Functionalized with Particles:

SEM was used to characterize the morphology of uniaxially aligned nanofibers functionalized with the particles in a density gradient. The average diameter of the nanofibers was then measured from 100 fibers in the SEM images. The water contact angles of different types of scaffolds were measured using a SL200A-type contact angle analyzer. The scaffolds consisting of uniaxially aligned nanofibers functionalized with FITC-BSA-loaded collagen particles were observed under a Leica DMI 6000 B inverted microscope. Five different positions with the same incremental distance along the fiber alignment were imaged. The average fluorescence intensities at each position were measured from three samples using ImageJ, and the relative fluorescence intensities as a function of distance along the aligned fibers were plotted.

Migration of Bone Marrow Stem Cells:

Rat bone marrow stem cells were cultured in α-MEM supplemented with 10% FBS and 1% ABAM. The migration of the cells on TCP and different types of scaffolds consisting of random nanofibers, aligned nanofibers, and aligned nanofibers coated with collagen particles in a uniform distribution or a unidirectional gradient were studied. Prior to use, the scaffolds were washed by cell culture media for three times. Then, a sterilized PDMS strip (length = 2.2 cm, width = 0.6 cm) was placed on the sample to leave a region with a width of 0.5 cm on the left side, and bone marrow stem cells were seeded at a concentration of 1×10^5 cells mL^{-1} on this region. In this case, only the left 1/4 of the sample was seeded with cells. After cell adhesion for 4 h, the strip was removed to allow the cells migrating forward. After incubation for another three days, the vinculin, F-actin, and nuclei of the cells were stained, respectively. Briefly, the cells were fixed in 3% glutaraldehyde solution for 10 min, permeabilized with 0.1% Triton X-100 for 5 min, and then blocked with 3% BSA solution for 1 h at room temperature. Afterwards, the samples were incubated in the staining solution containing Alexa Fluor 488 antivinculin for 3 h at 4 °C, followed by immersing in solutions of Alexa Fluor 555 phalloidin and 4′,6-diamidino-2-phenylindole (DAPI), respectively, for 20 and 5 min at room temperature. Between each two procedures, the samples were washed by PBS solution for three times. After staining, the samples were imaged under the laser confocal scanning microscope (Zeiss 700) using a tile mode. The distributions and morphologies of cells on the samples were observed from the micrographs taken at low and high magnifications, respectively. The numbers of cells in the migration zones of the samples were counted from the fluorescence micrographs of DAPI staining. The migration

distances of cells on the different samples were measured, and the migration speeds were calculated accordingly. Triplicate samples in each group were used for the study.

Migration of NIH-3T3 Fibroblasts:

The migration of NIH-3T3 fibroblasts on the aligned fibers functionalized with collagen particles in a bidirectional gradient, together with the random nanofibers, aligned nanofibers, and aligned nanofibers coated with collagen particles in a uniform distribution as control groups was investigated . Triplicate samples in each group were used for the study. NIH-3T3 fibroblasts were cultured in DMEM supplemented with 10% FBS and 1% ABAM. A PDMS strip (length = 2.2 cm, width = 0.6 cm) was placed on the center of the sample to generate a "wound" gap of 0.6 cm, and NIH-3T3 fibroblasts were seeded on both sides of the strip. After cell adhesion for 4 h, the strip was removed to allow the cell migrating from the two opposite sides toward the center. After incubation for another 3 d, the cells were fixed, stained, and then imaged using the similar protocols as described above for the BMSCs migration study. From the fluorescence micrographs, the numbers of cells in the migration zones and the migration distances of cells were measured, and the migration speeds of the collective cells were calculated accordingly.

Migration of Schwann Cells:

Schwann cells, isolated from rat sciatic nerves, were obtained commercially from ScienCell (catalog #R1700). The cells were cultured in the culture medium consisting of basal medium, 5% FBS, 1% cell growth supplement, and 1% ABAM. Those four groups used for culturing NIH-3T3 fibroblasts were also applied here to study the migration of Schwann cells from two opposites toward the center, except that the fibronectin was added into collagen to fabricate the particles. The same protocols were also used for culturing the cells and evaluating the outcome of cell migration by immunofluorescence staining and quantification analysis.

DRG Culture:

Embryonic day 8 (E8, stage HH35–36) chick was removed from the white leghorn egg. DRG cells were dissected from the thoracic region and collected in HBSS prior to plating. Afterwards, the DRG were seeded on the center of the samples (1 DRG per sample) in a modified neurobasal medium supplemented with 10% FBS, 1% N-2 supplement, and 1% ABAM. Three groups were prepared for incubating DRG: scaffolds consisting of aligned nanofibers, aligned nanofibers functionalized with the particles made of a mixture of collagen and laminin in a uniform distribution and a unidirectional density gradient, respectively. After culture for 6 d, the DRG cell bodies were fixed. The neurites were immunostained with Tuj1 primary antibody and Alexa Fluor 488 secondary antibody, and cell nuclei were stained with DAPI. Fluorescence micrographs were captured using a laser confocal scanning microscope. The average and the longest lengths of neurites extending from both sides of the DRG body were measured from the fluorescence micrographs. Six DRG cells on each type of scaffold were used to calculate the neurite length.

Statistical Analysis:

All the values were averaged at least in triplicate and presented in the form of mean ± standard deviation, with "n" indicating the number of samples per group. Comparison between groups was performed using one-way ANOVA, followed by Student's t-tests for all pairwise comparisons. Differences were considered statistically significant when $P < 0.05$.

Supplementary Material

Refer to Web version on PubMed Central for supplementary material.

Acknowledgements

This work was supported in part by a grant from the National Institutes of Health (R01 EB020050) and startup funds from the Georgia Institute of Technology.

References

[1]. Karimi F, O'Connor AJ, Qiao GG, Heath DE, Adv. Healthcare Mater 2018, 7, 1701324.
[2]. Li Q, Ma L, Gao C, J. Mater. Chem. B 2015, 3, 8921. [PubMed: 32263026]
[3]. Tracy LE, Minasian RA, Caterson EJ, Adv. Wound Care 2016, 5, 119.
[4]. Goodhill GJ, Trends Neurosci. 2016, 39, 202. [PubMed: 26927836]
[5]. Stevens MM, George JH, Science 2005, 310, 1135. [PubMed: 16293749]
[6]. Petrie RJ, Doyle AD, Yamada KM, Nat. Rev. Mol. Cell Biol 2009, 10, 538. [PubMed: 19603038]
[7]. Hoffman-Kim D, Mitchel JA, Bellamkonda RV, Annu. Rev. Biomed. Eng 2010, 12, 203. [PubMed: 20438370]
[8]. Vargas P, Barbier L, Sáez PJ, Piel M, Curr. Opin. Cell Biol 2017, 48, 72. [PubMed: 28641118]
[9]. Tocce EJ, Smirnov VK, Kibalov DS, Liliensiek SJ, Murphy CJ, Nealey PF, Biomaterials 2010, 31, 4064. [PubMed: 20153044]
[10]. Leclech C, Renner M, Villard C, Métin C, Biomaterials 2019, 214, 119194. [PubMed: 31154150]
[11]. Xie J, Liu W, MacEwan MR, Bridgman PC, Xia Y, ACS Nano 2014, 8, 1878. [PubMed: 24444076]
[12]. Seidi A, Ramalingam M, Elloumi-Hannachi I, Ostrovidov S, Khademhosseini A, Acta Biomater. 2011, 7, 1441. [PubMed: 21232635]
[13]. Bicknell BA, Pujic Z, Feldner J, Vetter I, Goodhill GJ, Sci. Data 2018, 5, 180183. [PubMed: 30179228]
[14]. Chang Y-C, Chen M-H, Liao S-Y, Wu H-C, Kuan C-H, Sun J-S, Wang T-W, ACS Appl. Mater. Interfaces 2017, 9, 37623. [PubMed: 28990762]
[15]. Tanes ML, Xue J, Xia Y, J. Mater. Chem. B 2017, 5, 5580. [PubMed: 28848651]
[16]. Li X, Xie J, Lipner J, Yuan X, Thomopoulos S, Xia Y, Nano Lett. 2009, 9, 2763. [PubMed: 19537737]
[17]. Lipner J, Liu W, Liu Y, Boyle J, Genin GM, Xia Y, Thomopoulos S, J. Mech. Behav. Biomed. Mater 2014, 40, 59. [PubMed: 25194525]
[18]. Liu W, Lipner J, Xie J, Manning CN, Thomopoulos S, Xia Y, ACS Appl. Mater. Interfaces 2014, 6, 2842. [PubMed: 24433042]
[19]. Liu W, Zhang Y, Thomopoulos S, Xia Y, Angew. Chem 2013, 125, 447.
[20]. Xue J, Xie J, Liu W, Xia Y, Acc. Chem. Res 2017, 50, 1976. [PubMed: 28777535]
[21]. Chen S, Li R, Li X, Xie J, Adv. Drug Delivery Rev 2018, 132, 188.
[22]. Li X, Chen Z, Zhang H, Zhuang Y, Shen H, Chen Y, Zhao Y, Chen B, Xiao Z, Dai J, Polymers 2019, 11, 341.
[23]. Han J, Xiong L, Jiang X, Yuan X, Zhao Y, Yang D, Prog. Polym. Sci 2019, 91, 1.

[24]. Liu W, Thomopoulos S, Xia Y, Adv. Healthcare Mater 2012, 1, 10.
[25]. Xue J, Wu T, Xia Y, APL Mater. 2018, 6, 120902.
[26]. Ottosson M, Jakobsson A, Johansson F, PLoS One 2017, 12, e0169419. [PubMed: 28060880]
[27]. Xie J, MacEwan MR, Schwartz AG, Xia Y, Nanoscale 2010, 2, 35. [PubMed: 20648362]
[28]. Xie J, MacEwan MR, Liu W, Jesuraj N, Li X, Hunter D, Xia Y, ACS Appl. Mater. Interfaces 2014, 6, 9472. [PubMed: 24806389]
[29]. Shi J, Wang L, Zhang F, Li H, Lei L, Liu L, Chen Y, ACS Appl. Mater. Interfaces 2010, 2, 1025. [PubMed: 20423122]
[30]. Sundararaghavan HG, Saunders RL, Hammer DA, Burdick JA, Biotechnol. Bioeng 2013, 110, 1249. [PubMed: 23172355]
[31]. Wu T, Xue J, Li H, Zhu C, Mo X, Xia Y, ACS Appl. Mater. Interfaces 2018, 10, 8536. [PubMed: 29420008]
[32]. Wu S, Du W, Duan Y, Zhang D, Liu Y, Wu B, Zou X, Ouyang H, Gao C, Acta Biomater. 2018, 75, 75. [PubMed: 29857130]
[33]. Yu S, Zuo X, Shen T, Duan Y, Mao Z, Gao C, Acta Biomater. 2018, 72, 70. [PubMed: 29635070]
[34]. Liang S, Yu S, Zhou N, Deng J, Gao C, Acta Biomater. 2017, 56, 161. [PubMed: 27998813]
[35]. Xie J, Jiang J, Davoodi P, Srinivasan MP, Wang C-H, Chem. Eng. Sci 2015, 125, 32. [PubMed: 25684778]
[36]. Boda SK, Li X, Xie J, J. Aerosol Sci 2018, 125, 164. [PubMed: 30662086]
[37]. Somaiah C, Kumar A, Mawrie D, Sharma A, Patil SD, Bhattacharyya J, Swaminathan R, Jaganathan BG, PLoS One 2015, 10, e0145068. [PubMed: 26661657]
[38]. Choi S, Friedrichs J, Song YH, Werner C, Estroff LA, Fischbach C, Biomaterials 2019, 198, 95. [PubMed: 29759731]
[39]. Plantman S, Patarroyo M, Fried K, Domogatskaya A, Tryggvason K, Hammarberg H, Cullheim S, Mol. Cell. Neurosci 2008, 39, 50. [PubMed: 18590826]
[40]. Armstrong SJ, Wiberg M, Terenghi G, Kingham PJ, Tissue Eng. 2007, 13, 2863. [PubMed: 17727337]
[41]. Li X, MacEwan MR, Xie J, Siewe D, Yuan X, Xia Y, Adv. Funct. Mater 2010, 20, 1632. [PubMed: 21687818]
[42]. Gupta P, Elkins C, Long TE, Wilkes GL, Polymer 2005, 46, 4799.
[43]. Bock N, Dargaville TR, Woodruff MA, Prog. Polym. Sci 2012, 37, 1510.
[44]. He L, Theato P, Eur. Polym. J 2013, 49, 2986.
[45]. Luque G, Stürtz R, Passeggi M, Gugliotta L, Gonzalez D, Minari R, Int. J. Adhes. Adhes 2020, 100, 102624.
[46]. Link PA, Tissue Eng J. Regener. Med 2018, 12, 2331.
[47]. Palumbo R, Galvez BG, Pusterla T, De Marchis F, Cossu G, Marcu KB, Bianchi ME, J. Cell Biol 2007, 179, 33. [PubMed: 17923528]
[48]. Hocking AM, Adv. Wound Care 2015, 4, 623.
[49]. Cao J, Wang L, Du Z-J, Liu P, Zhang Y-B, Sui J-F, Liu Y-P, Lei D-L, Br. J. Oral Maxillofac. Surg 2013, 51, 937. [PubMed: 23747231]
[50]. Arnold M, Schwieder M, Blümmel J, Cavalcanti-Adam EA, López-Garcia M, Kessler H, Geiger B, Spatz JP, Soft Matter 2009, 5, 72. [PubMed: 21686049]
[51]. Mi H-Y, Salick MR, Jing X, Crone WC, Peng X-F, Turng L-S, J. Biomed. Mater. Res., Part A 2015, 103, 593.
[52]. Nelson T, Short A, Cole S, Gross A, Winter J, Eubank T, Lannutti J, BMC Cancer 2014, 14, 825. [PubMed: 25385001]
[53]. Ren X, Han Y, Wang J, Jiang Y, Yi Z, Xu H, Ke Q, Acta Biomater. 2018, 70, 140. [PubMed: 29454159]
[54]. Cattin A-L, Burden JJ, Emmenis LV, Mackenzie FE, Hoving JA, Calavia NG, Guo Y, McLaughlin M, Rosenberg LH, Quereda V, Jamecna D, Napoli I, Parrinello S, Enver T, Ruhrberg C, Lloyd AC, Cell 2015, 162, 1127. [PubMed: 26279190]

[55]. Magaz A, Faroni A, Gough JE, Reid AJ, Li X, Blaker JJ, Adv. Healthcare Mater 2018, 7, 1800308.

[56]. Mortimer D, Feldner J, Vaughan T, Vetter I, Pujic Z, Rosoff WJ, Burrage K, Dayan P, Richards LJ, Goodhill GJ, Proc. Natl. Acad. Sci. USA 2009, 106, 10296. [PubMed: 19541606]

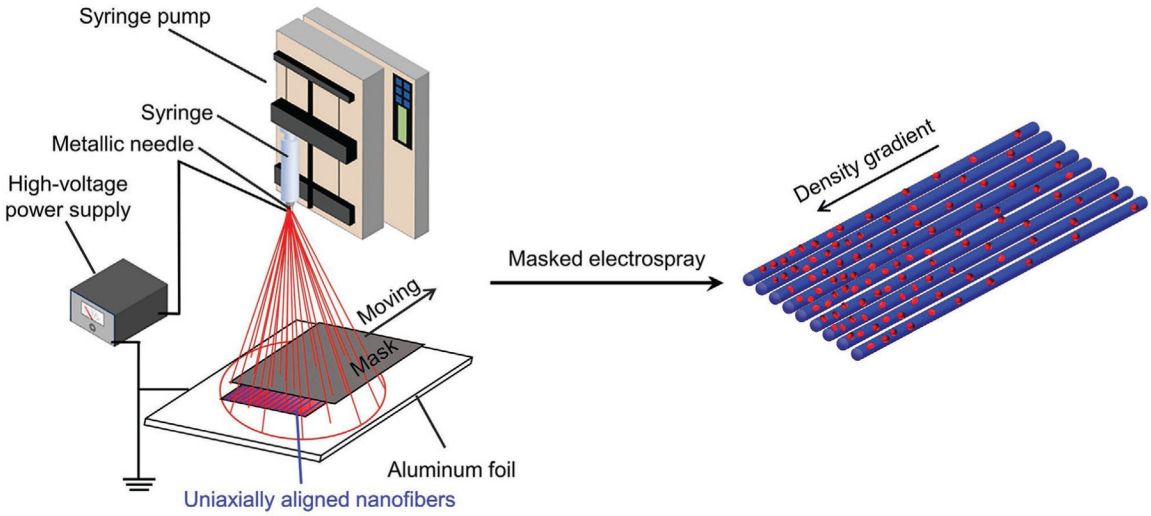

Figure 1.

A schematic of the setup used for depositing biomacromolecular particles on uniaxially aligned nanofibers in a unidirectional density gradient via masked electrospray. The mask above the fibers moves at a constant speed to vary the collection time along the fiber alignment. A bidirectional density gradient of particles that increases from two opposite sides to the center can be fabricated by completely blocking half of the scaffold while collecting the particles on the other half, followed by reverting the process.

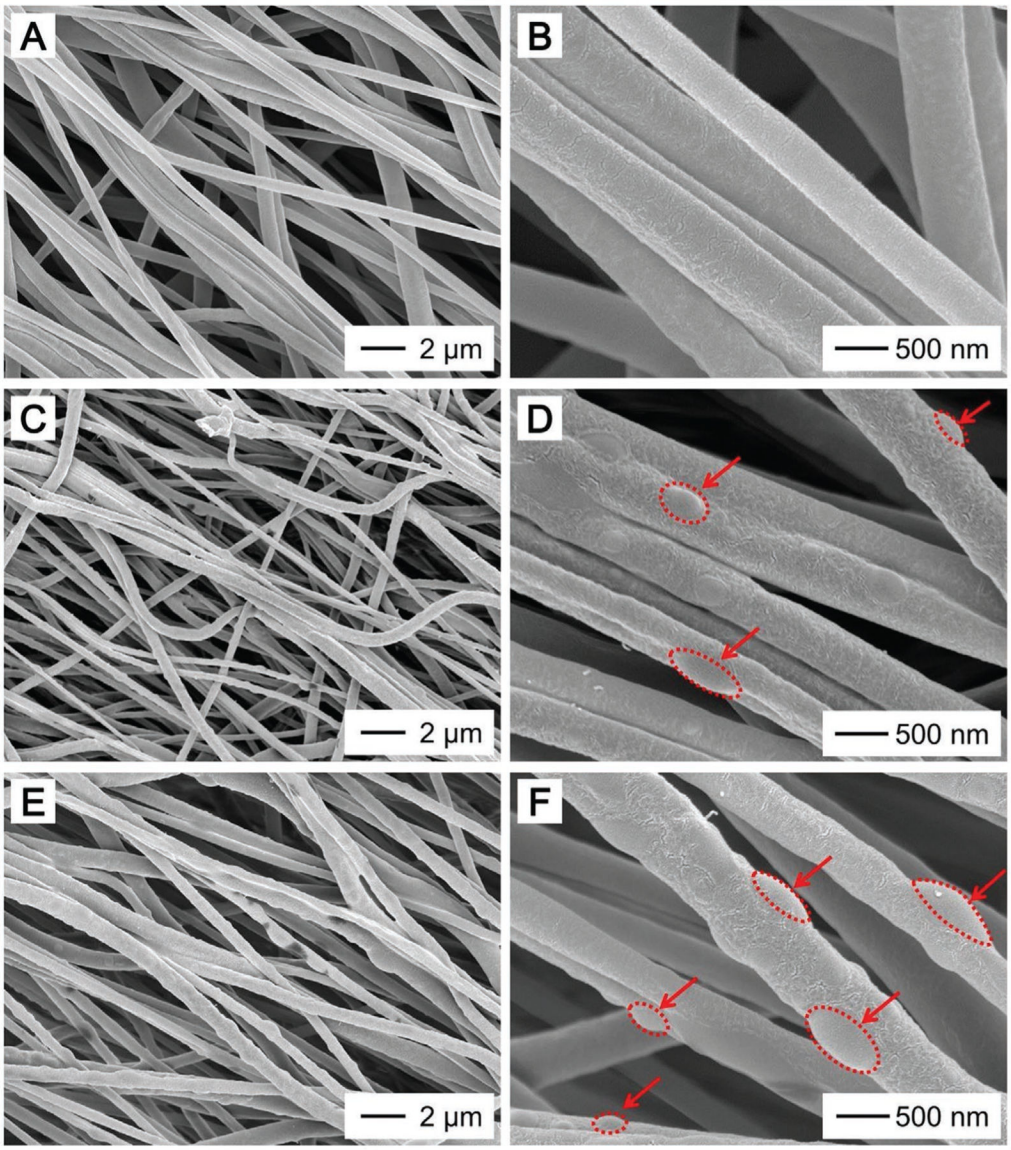

Figure 2.

SEM images of uniaxially aligned nanofibers whose surfaces were functionalized with collagen particles (marked by red dotted ellipses together with the arrows) at positions that correspond to collection times of A,B) 0, C,D) 10, and E,F) 20 min, respectively.

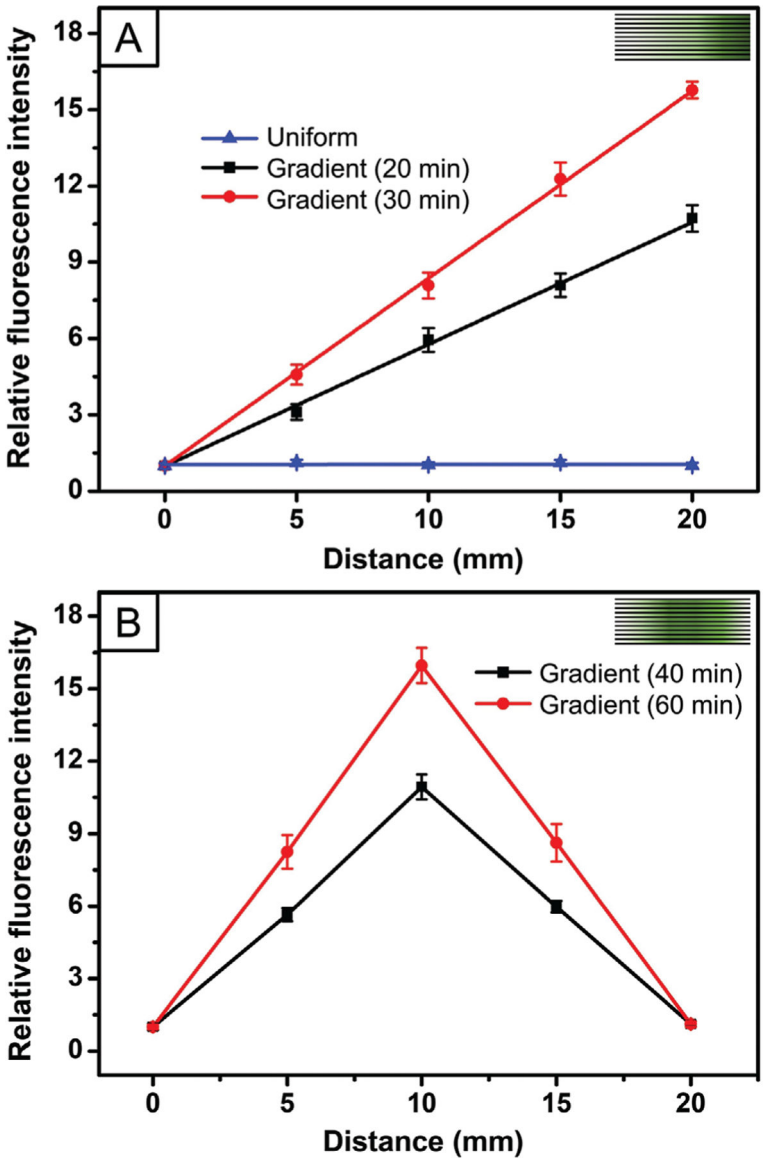

Figure 3.

Plots of relative fluorescence intensities as a function of distance along the direction of gradient for FITC-BSA-loaded collagen particles deposited on the aligned nanofibers in a A) uniform distribution and a unidirectional gradient, and B) a bidirectional gradient, respectively. The slope of the line can be adjusted by varying the moving speed of the mask. The insets in A,B) illustrate the unidirectional and bidirectional gradients, respectively. The distance refers to the distance away from the edge of the fiber scaffold where the collagen particles were deposited for 2 min.

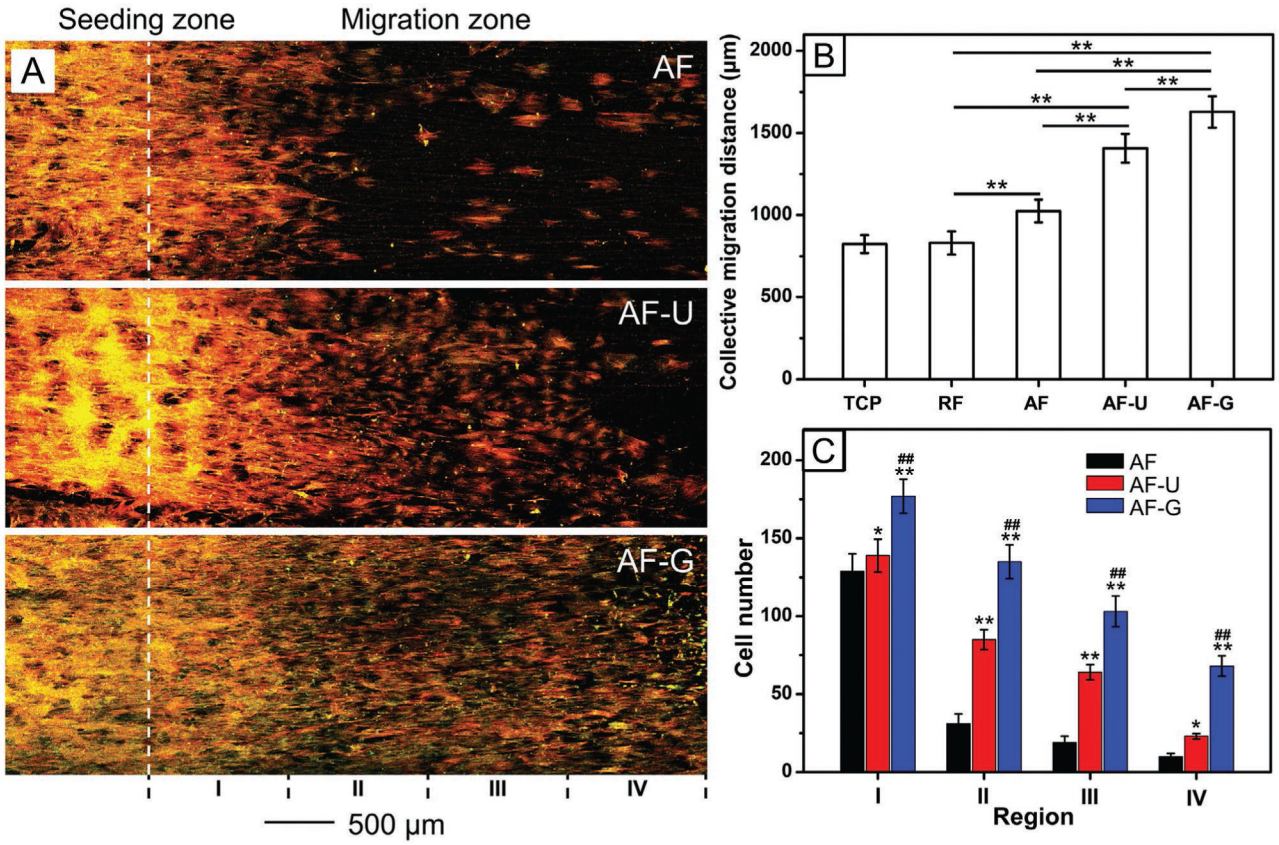

Figure 4.

A) Fluorescence micrographs showing the migration of bone marrow stem cells on the different types of scaffolds consisting of aligned nanofibers (AF), aligned nanofibers coated with collagen particles in a uniform distribution (AF-U), and aligned nanofibers deposited with collagen particles in a unidirectional gradient (AF-G). The actin cytoskeleton was stained with Alexa Fluor 555 phalloidin (red) and the vinculin was stained with Alexa Fluor 488 antivinculin (green). The yellow color corresponds to an overlay of these two colors. Analysis of the migration behavior of bone marrow stem cells on the different types of scaffolds. B) The collective migration distance of bone marrow stem cells on different types of scaffolds. $^{**}P < 0.01$. C) The number of stem cells within an area of 1 mm^2 at different regions of the migration zone on the different types of scaffolds. $^{*}P < 0.05$ and $^{**}P < 0.01$ when compared to the group of AF. $^{\#\#}P < 0.01$ when compared to the group of AF-U ($n = 3$).

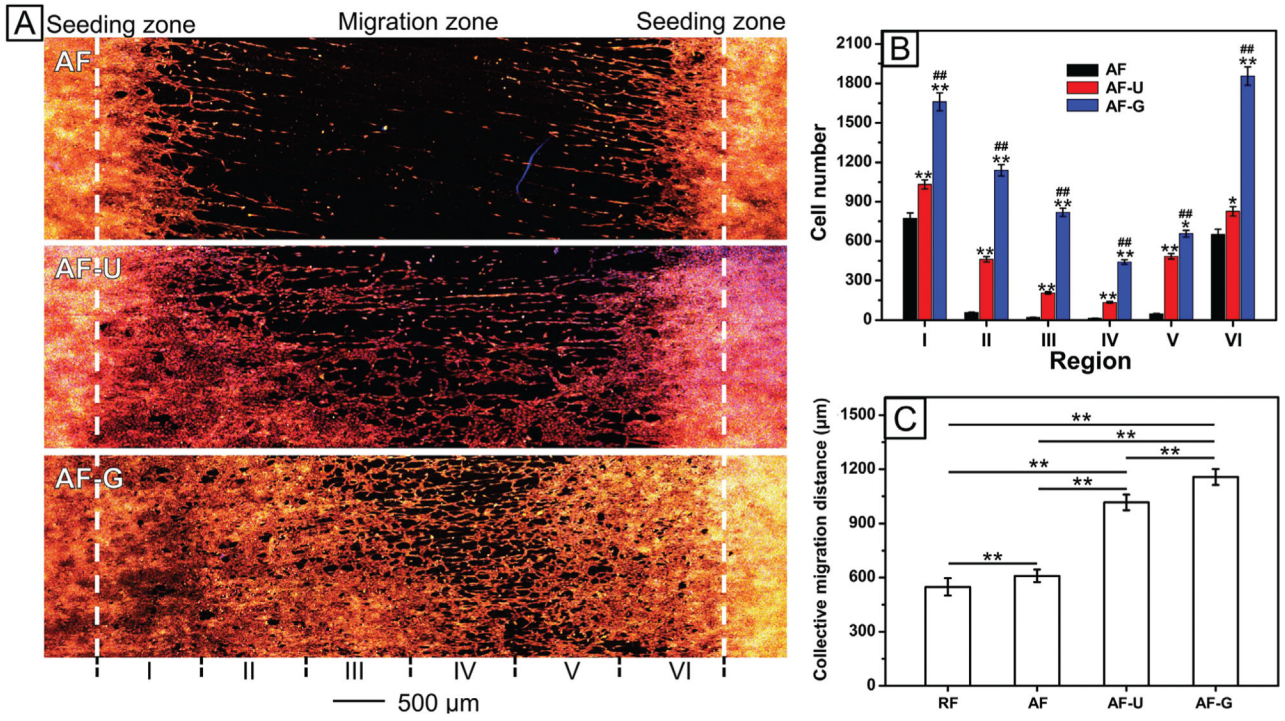

Figure 5.

A) Fluorescence micrographs showing the migration of NIH-3T3 fibroblasts from the two sides toward the center on the different types of scaffolds after culture for three days. The actin cytoskeleton and the vinculin were stained with Alexa Fluor 555 phalloidin (red) and Alexa Fluor 488 antivinculin (green), respectively. The yellow color corresponds to an overlay of these two colors. Analysis of the migration behavior of NIH-3T3 fibroblasts on the different types of scaffolds. B) The number of fibroblasts within an area of 1 mm^2 at different regions of the migration zones on the different types of scaffolds. $^{*}P < 0.05$ and $^{**}P < 0.01$ when compared to the group of AF. $^{\#\#}P < 0.01$ when compared to the group of AF-U ($n = 3$). C) The collective migration distance of NIH-3T3 fibroblasts on different types of scaffolds. $^{**}P < 0.01$.

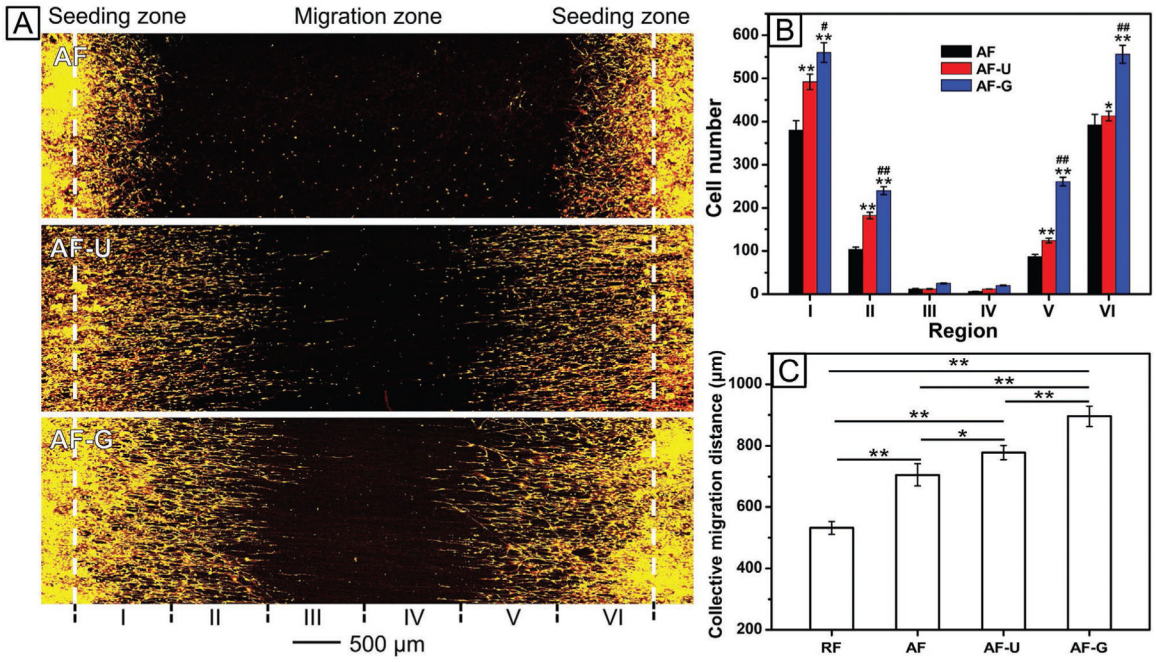

Figure 6.

A) Fluorescence micrographs showing the migration of Schwann cells from the two sides toward the center on the different types of scaffolds after culture for three days. The actin cytoskeleton and the vinculin were stained with Alexa Fluor 555 phalloidin (red) and Alexa Fluor 488 antivinculin (green), respectively. The yellow color corresponds to an overlay of these two colors. Analysis of the migration behavior of Schwann cells on the different types of scaffolds. B) The number of cells within an area of 1 mm^2 at different regions of the migration zones on the different types of scaffolds. $^{*}P < 0.05$ and $^{**}P < 0.01$ when compared to the group of AF. $^{\#\#}P < 0.01$ when compared to the group of AF-U ($n = 3$). C) The collective migration distance of Schwann cells on the different types of scaffolds. $^{**}P < 0.01$ and $^{*}P < 0.05$.

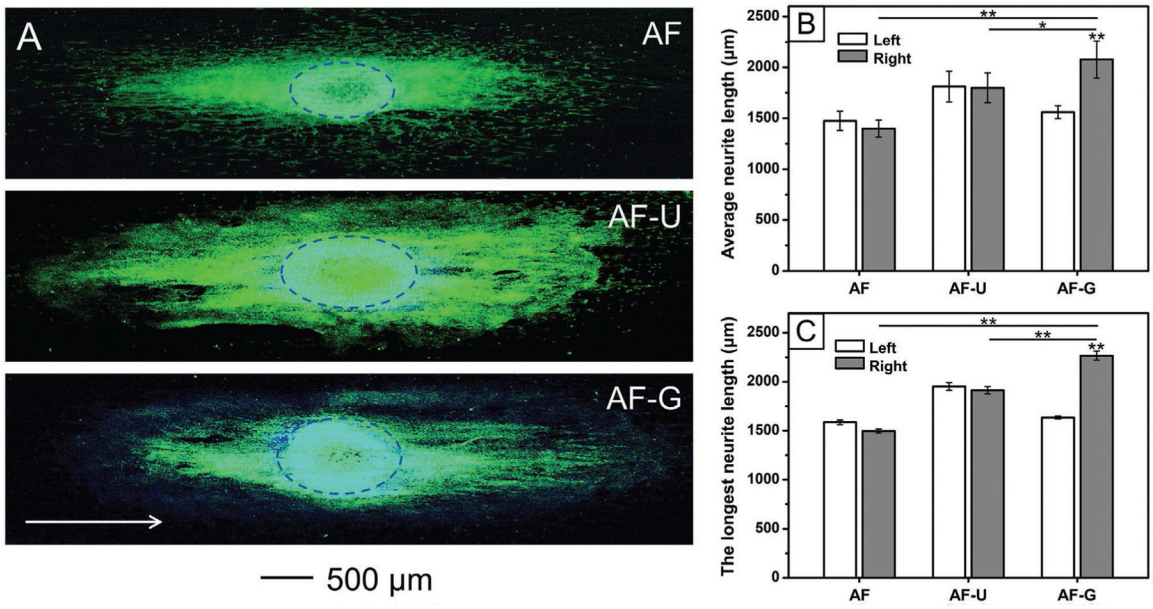

Figure 7.

A) Fluorescence micrographs showing the neurites extending from DRG bodies when cultured on the different types of scaffolds for six days. The neurites and the nuclei were stained with Tuj1 (green) and DAPI (blue), respectively. The white arrow indicates the direction of increasing particle density. B) The average and C) the longest lengths of neurites extending from the left and right sides of the DRG when cultured on the different types of scaffolds. $*P < 0.05$ and $**P < 0.01$.